NUMERICAL CHARACTERIZATION OF BISTATIC SCATTERING FROM PEC CYLINDER PARTIALLY EMBEDDED IN A DIELECTRIC ROUGH SURFACE INTERFACE: HORIZONTAL POLARIZATION

X. Wang

Department of Electrical Engineering
The Pennsylvania State University
University Park, PA 16802, USA

L.-W. Li

Department of Electrical and Computer Engineering
National University of Singapore
10 Kent Ridge Crescent, Singapore 119260, Singapore

Abstract—Scattering from a two-dimensional (2-D) perfectly electrically conducting (PEC) cylinder partially embedded in a random dielectric rough surface interface is studied using the method of moments (MoM) with pulse basis functions and the point matching technique, for the case of horizontal polarization. The random rough surface is modeled using Gaussian statistical characteristic for the rough surface height and surface correlation function, and generated by the spectral-method. The tapered plane-wave incidence is used to avoid artificial edge diffraction due to the truncation of the rough surface into finite-length rough surface in the numerical simulations. With the developed algorithms, the interactions between the dielectric rough surface and the partially buried PEC cylinder are investigated using the Monte Carlo simulation, and are expressed as a function of the root mean square (rms) height of a random dielectric rough surface and the moisture content of the soil. The numerical results show that the bistatic scattering coefficients are dependent upon the moisture content, the rms height of a rough surface, and other parameters.

Corresponding author: X. Wang (XUW11@psu.edu).

1. INTRODUCTION

Electromagnetic scattering by objects located entirely above or below a rough surface has been extensively studied using analytical and numerical methods, primarily due to its wide applications in microwave remote sensing and radar signature. However, many realistic scattering applications involve targets located in complicated environments, for instance, partially embedded in a semi-infinite dielectric ground plane. Accurately characterizing the interactions between the dielectric surface and the partially buried targets is especially an important objective for the analysis of the electromagnetic wave scattering from a ship on ocean where the statistic property of the scattering cross section is necessary and should be thus studied. The interface of the semi-infinite dielectric ground plane is usually assumed to be a planar interface, so as to simplify mathematically the problem of interest. As compared to those modeled assuming a planar surface, however, the surface roughness of the ground interface could significantly affect the target's scattering properties, particularly when the roughness is larger than a fraction of the electromagnetic wavelength. Thus, more accurate modeling of the aforementioned complicated but practical environment is required, taking into account the effects of the rough surface interface on the object's scattering property. This thus motivates the present paper and forms the primary objective to be achieved.

Electromagnetic scattering by three-dimensional (3-D) objects located above a dielectric rough surface with a small roughness limit has been investigated using an analytical method [1–3]. The analytical algorithm has also been applied to solve the problem of scattering by 2-D dielectric circular cylinder under beneath a slightly rough surface [4]. The advantage of the analytical method is the computational simplicity. The results obtained can be used to serve as benchmarks for numerical algorithms. The scattering mechanisms and physical significance can also be easily understood from the analytical solutions. The disadvantage of the analytical method is its applicability limited to canonical geometries, and to a small rms rough surface height. Therefore, a numerical method has to be used to characterize the electromagnetic scattering from general targets located above or below a dielectric rough surface. The scattering by a 2-D dielectric circular cylinder buried below a sinusoidal interface has been discussed in [5] and [6] using an integral equation with the extended boundary condition method. The MoM with pulse basis functions and the point matching technique have been proposed to evaluate the wave scattering by a 2-D PEC circular cylinder located above or below

a random dielectric rough surface for TE (horizontal polarization) [8] and TM (vertical polarization) [9, 28] cases. For a 3-D PEC spherical scatterer under a 2-D random dielectric rough surface, the problem has been solved using the MoM based on surface integral equations [10]. The MoM and modified PO hybrid method has been used to analysis of scattering from 3-D PEC object buried under rough surface [29]. To accelerate the solution to the electromagnetic scattering by a 3-D dielectric/PEC object located above or below a 2-D dielectric rough surface, the coupled canonical grid and discrete dipole approach (DDA) [11] and the steepest descent fast multipole method (SDFMM) [12] have been carried out. In addition, time-domain algorithm such as the finite-difference time-domain (FDTD) technique has also been employed to analyze the electromagnetic scattering by a 2-D metallic cylinder under a random dielectric rough surface [7].

Scattering from a 2-D (or 3-D) scatterer partially embedded in a planar semi-infinite PEC ground plane has also been studied by other researchers. The image method has been used to solve this problem, under plane wave illumination in the 2-D [13, 14] and 3-D [15] cases. The MoM [16] and the finite-difference method [17] have also been applied to analyze the electromagnetic scattering by a 2-D PEC cylinder partially buried at flat dielectric interface. The generalized forward-backward (GFB) method has been employed to analyze scattering by 2-D objects on ocean-like rough surface to obtain accurate results and a fast convergence in an iterative procedure [18, 19], where both targets and rough surface are assumed to be metallic.

However, the electromagnetic scattering of objects partially embedded in a random dielectric rough surface interface is neither well studied nor documented in literature, to our knowledge. We investigate the electromagnetic scattering by a 2-D metallic cylinder partially buried in a dielectric rough surface interface in the TM case [20]. Recently, a hybrid approach of the forward-backward method (FBM) with spectral accelerate algorithm (SAA) and Monte Carlo method has been developed for analysis of scattering from rough dielectric soil surface with a conducting object partially buried [30]. In this paper, the algorithm proposed in [20] is extended to deal with the electromagnetic scattering of PEC cylinder partially embedded in dielectric rough surface, for the case of horizontal polarization (TE case). The present paper is distinct from [20] in that: (1) the different polarization (horizontal polarization) is considered in the present work, (2) the formulas are described in detail as compared to [20, 30], and (3) more examples are considered and more detailed explanations of the observed phenomena are presented. It should be noted that various

terminologies are used literature to define the polarization. Here, H-polarization (or TE case) is used, as defined in the same coordinates in [25, pp. 115], for the Dirichlet boundary condition in the area of remote sensing.

This paper is organized as follows. Detailed derivation of the integral equations on the basis of the boundary condition and the resultant matrix equations are described in Section 2. The numerical results based on the Monte Carlo simulations are presented in Section 3 as a function of the surface roughness, the moisture content of the soil, and objects location. The properties of bistatic scattering coefficients for the 2-D PEC cylinder partially embedded in a random dielectric rough surface interface are also discussed in the section. Finally, conclusions and remarks are given in Section 4.

2. PROBLEM FORMULATION

2.1. The Random Rough Surface Generation

The spectral method proposed in [21] is applied to generate the random rough surface geometry with the Gaussian statistic characteristic for the rough surface height and surface correlation function. This kind of statistical rough surface modeling is often used elsewhere in literature for computation of electromagnetic wave scattered by a random rough surface. To analyze the interaction between dielectric random rough surface and PEC targets partially buried in a rough surface, truncation of the rough surface into finite-length rough surface is required from the numerical approach point of view. In order to reduce the artificial end effects introduced by the finite-length rough surface, the tapered plane wave illumination is assumed. So, bistatic scattering coefficients can be computed using the MoM, based on a large number of realizations of the Monte Carlo trials.

2.2. Integral Equations: Horizontal Polarization

Figure 1 shows the configuration for the wave scattering by a 2-D PEC cylinder partially embedded in a dielectric rough surface interface. The upper half-space and the lower half-space of the random rough surface are denoted as region 0 and region 1, respectively, and characterized by (μ_0, ε_0) and (μ_1, ε_1), correspondingly; with $\varepsilon_1 = \varepsilon_r \varepsilon_0$. E_y^{inc} denoting the incident electric field. $E_{y0}(\mathbf{r})$ and $E_{y1}(\mathbf{r})$ represent the scattered electric fields in region 0 and transmitted electric field region 1, respectively.

As mentioned above and described in [20], to avoid the artificial edge diffraction, the incident field used is the tapered plane wave,

instead of plane wave. The tapered plane wave is introduced in [21] and it satisfies the Maxwell's equations in an approximate sense. Considering a one-dimensional (1-D) random rough surface described by $z = Z(x)$ with a Gaussian correlation function, the tapered plane wave incident on the 1-D random rough surface can be expressed as follows

$$E_y^{inc}(\mathbf{r}) = \exp[ik_0(x\sin\theta_i - z\cos\theta_i)(1+w(\mathbf{r}))] \times \exp\left[-(x+z\tan\theta_i)^2/g^2\right] \tag{1}$$

where $w(\mathbf{r}) = [2(x + z\tan\theta_i)^2/g^2 - 1]/(k_0 g\cos\theta_i)^2$. The time dependence $\exp(-i\omega t)$ is assumed and suppressed. The incident angle θ_i is defined with respect to the normal in the counterclockwise direction and g is the tapering parameter with a length controlling the tapering of the incident wave. The g is usually chosen to be a value between $L/4$ to $L/10$, depending on the incident angle for the case of finite-length rough surface scattering. The L is the rough surface length. The presence of $w(\mathbf{r})$ in (1) ensures that E_y^{inc} satisfies the wave equation to the order of $1/(k_0 g\cos\theta_i)^2$, where $k_0 g\cos\theta_i \gg 1$ [21]. Thus, care should be taken when using E_y^{inc} for problems with low grazing angle (LGA) of incidence.

The electric fields on the dielectric rough surface and the 2-D PEC cylinder's surface satisfy the boundary conditions in region 0 and
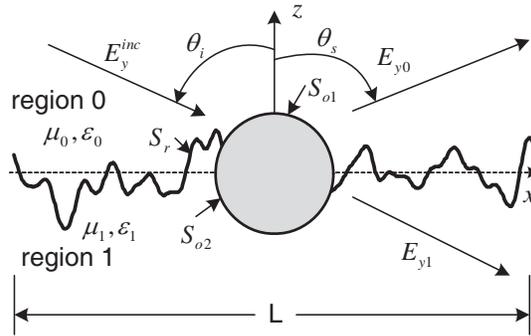
Figure 1. Geometry of the scattering problem.

region 1 as follows,

$$\frac{1}{2}E_{y0}(\mathbf{r}) = E_y^{inc}(\mathbf{r}) + \int_{s_r} \left[E_{y0}(\mathbf{r}')\frac{\partial G_0(\mathbf{r},\mathbf{r}')}{\partial n'} - G_0(\mathbf{r},\mathbf{r}')\frac{\partial E_{y0}(\mathbf{r}')}{\partial n'} \right] ds'$$
$$- \int_{s_{o1}} G_0(\mathbf{r},\mathbf{r}')\frac{\partial E_{y0}(\mathbf{r}')}{\partial n'} ds' \quad \mathbf{r} \in S_r \tag{2}$$

$$0 = E_y^{inc}(\mathbf{r}) + \int_{s_r} \left[E_{y0}(\mathbf{r}')\frac{\partial G_0(\mathbf{r},\mathbf{r}')}{\partial n'} - G_0(\mathbf{r},\mathbf{r}')\frac{\partial E_{y0}(\mathbf{r}')}{\partial n'} \right] ds'$$
$$- \int_{s_{o1}} G_0(\mathbf{r},\mathbf{r}')\frac{\partial E_{y0}(\mathbf{r}')}{\partial n'} ds' \quad \mathbf{r} \in S_{o1} \tag{3}$$

$$\frac{1}{2}E_{y1}(\mathbf{r}) = -\int_{s_r} \left[E_{y1}(\mathbf{r}')\frac{\partial G_1(\mathbf{r},\mathbf{r}')}{\partial n'} - G_1(\mathbf{r},\mathbf{r}')\frac{\partial E_{y1}(\mathbf{r}')}{\partial n'} \right] ds'$$
$$+ \int_{s_{o2}} G_1(\mathbf{r},\mathbf{r}')\frac{\partial E_{y1}(\mathbf{r}')}{\partial n'} ds' \quad \mathbf{r} \in S_r \tag{4}$$

$$0 = -\int_{s_r} \left[E_{y1}(\mathbf{r}')\frac{\partial G_1(\mathbf{r},\mathbf{r}')}{\partial n'} - G_1(\mathbf{r},\mathbf{r}')\frac{\partial E_{y1}(\mathbf{r}')}{\partial n'} \right] ds'$$
$$+ \int_{s_{o2}} G_1(\mathbf{r},\mathbf{r}')\frac{\partial E_{y1}(\mathbf{r}')}{\partial n'} ds' \quad \mathbf{r} \in S_{o2} \tag{5}$$

where S_r, S_{o1} and S_{o2} stand for the rough surface, the PEC cylinder's surfaces in the upper region 0 and the lower region 1, respectively. $G_0(\mathbf{r},\mathbf{r}')$ and $G_1(\mathbf{r},\mathbf{r}')$ are the Green's functions in region 0 and region 1 as given in [20], respectively. k_0 and $k_1 = \omega\sqrt{\mu_1\varepsilon_1}$ are the wavenumber in the upper region 0 and the lower region 1, respectively. For $\mathbf{r} \in S_r$, the electric fields $E_{y0}(\mathbf{r})$ and $E_{y1}(\mathbf{r})$ on the dielectric rough surface satisfy the following boundary conditions

$$E_{y0}(\mathbf{r})|_{\mathbf{r}\in S_r} = E_{y1}(\mathbf{r})|_{\mathbf{r}\in S_r} \tag{6}$$
$$\left.\frac{E_{y0}(\mathbf{r})}{\partial n}\right|_{\mathbf{r}\in S_r} = \frac{1}{\rho}\left.\frac{\partial E_{y1}(\mathbf{r})}{\partial n}\right|_{\mathbf{r}\in S_r} \tag{7}$$

where $\rho = \mu_1/\mu_0$. The normal derivative of the 2-D Green's function can be found in [20]. The difference between integral equations for the TE case considered here and the TM case in [20] is the components representing the scattered field from partially buried target. Please note that expression of coefficient ρ appeared in Eq. (7) is also different from that in Eq. (4) of [20]. The integral equations in (2)–(5) are converted into matrix equations by using the MoM with pulse basis

functions and the point matching technique, with discretization on the dielectric rough surface S_r and the PEC cylinder's surface S_o (including both the S_{o1} and the S_{o2}). The resultant matrix equations are given as

$$
\begin{bmatrix}
A & B & C & 0 \\
D & -\rho E & 0 & F \\
G & H & I & 0 \\
J & -\rho K & 0 & L
\end{bmatrix}
\begin{bmatrix}
V_1 \\
V_2 \\
V_3 \\
V_4
\end{bmatrix}
=
\begin{bmatrix}
E_y^{inc} \\
0 \\
E_{yo1}^{inc} \\
0
\end{bmatrix}
\tag{8}
$$

where $V_1(x) = E_{y0}(\vec{r})|_{\vec{r} \in S_r}$, $V_2(x) = \partial E_{y0}/\partial n|_{x \in S_r}$, $V_3(x) = E_{y0}|_{x \in S_{o1}}$, and $V_4(x) = E_{y0}|_{x \in S_{o2}}$. E_y^{inc} denotes the incident electric field on the rough surface S_r, while E_{yo1}^{inc} represents the incident electric field on the upper PEC cylinder's surface S_{o1} in region 0. Formulas for the elements A, B, D and E of the block impedance matrix are the same as those appearing in [20]. The other block impedance matrices are given by,

$$
C_{mq} = \gamma_{o1q} \Delta x (i/4) H_0^{(1)} \left(k_0 |\mathbf{r}_m - \mathbf{r}_{o1q}| \right) \tag{9}
$$

$$
F_{mv} = -\gamma_{o2v} \Delta x (i/4) H_0^{(1)} \left(k_1 |\mathbf{r}_m - \mathbf{r}_{o2v}| \right) \tag{10}
$$

$$
G_{pn} = -\gamma_n \Delta x \left(i k_0/4 \right) \left(\hat{\mathbf{n}} \cdot \mathbf{R}_1 \right) H_1^{(1)} \left(k_0 |\mathbf{r}_{o1p} - \mathbf{r}_n| \right) \tag{11}
$$

$$
H_{pn} = \gamma_n \Delta x (i/4) H_0^{(1)} \left(k_0 |\mathbf{r}_{o1p} - \mathbf{r}_n| \right) \tag{12}
$$

$$
I_{pq} = \begin{cases}
\gamma_{o1q} \Delta x (i/4) H_0^{(1)} \left(k_0 |\mathbf{r}_{o1p} - \mathbf{r}_{o1q}| \right), & p \neq q \\
\gamma_{o1q} \Delta x (i/4) H_0^{(1)} \left[k_0 \Delta x \gamma_{o1q}/(2e) \right], & p = q
\end{cases} \tag{13}
$$

$$
J_{un} = \gamma_n \Delta x \left(i k_1/4 \right) \left(\hat{\mathbf{n}} \cdot \mathbf{R}_2 \right) H_1^{(1)} \left(k_1 |\mathbf{r}_{o2u} - \mathbf{r}_n| \right) \tag{14}
$$

$$
K_{un} = \gamma_n \Delta x (i/4) H_0^{(1)} \left(k_1 |\mathbf{r}_{o2u} - \mathbf{r}_n| \right) \tag{15}
$$

$$
Q_{uv} = \begin{cases}
\gamma_{o2v} \Delta x (i/4) H_0^{(1)} (k_1 |\mathbf{r}_{o2u} - \mathbf{r}_{o2v}|), & u \neq v \\
\gamma_{o2v} \Delta x (i/4) H_0^{(1)} \left[k_1 \Delta x \gamma_{o2v}/(2e) \right], & u = v
\end{cases} \tag{16}
$$

where $\hat{\mathbf{n}}$ is normal vector of surface considered, $\mathbf{R}_1 = (\mathbf{r}_{o1p} - \mathbf{r}_n)/|\mathbf{r}_{o1p} - \mathbf{r}_n|$, $\mathbf{R}_2 = (\mathbf{r}_{o2v} - \mathbf{r}_n)/|\mathbf{r}_{o2v} - \mathbf{r}_n|$, $e = 2.71828138$, $\gamma_n = \sqrt{1 + [Z'(x_n)]^2}$, $\gamma_{o1p} = \sqrt{1 + [Z'_{o1}(x_{o1p})]^2}$, $\gamma_{o2v} = \sqrt{1 + [Z'_{o2}(x_{o2v})]^2}$, and $\{\mathbf{r}_m, \mathbf{r}_n\} \in S_r$, $\{\mathbf{r}_{o1q}, \mathbf{r}_{o1p}\} \in S_{o1}$, $\{\mathbf{r}_{o2u}, \mathbf{r}_{o2v}\} \in S_{o2}$. $Z'(x_n)$ is the first-order derivatives of the rough surface height profile function $Z(x_n)$. $Z'_{o1p}(x_{o1p})$ and $Z'_{o2v}(x_{o2v})$ are the first-order derivative of the cylinder's surface profile function located on S_{o1} and S_{o2}, respectively.

The far-zone scattered field in the upper region 0 can be calculated once the matrix equation in (8) is solved. The normalized bistatic scattering coefficient is given as follows for the tapered wave

incidence [22]:

$$\sigma(\theta_s) = |E_{ys}(\theta_s, \theta_i)|^2 \bigg/ \left[g\sqrt{\pi/2}\cos\theta_i \left(1 - \frac{1 + 2\tan^2\theta_i}{2k_0^2 g^2 \cos^2\theta_i}\right)\right] \quad (17)$$

where

$$
\begin{aligned}
E_{ys}(\theta_s, \theta_i) = {} & (i/4)\sqrt{2/(\pi k_0)}e^{-i\pi/4} \cdot \bigg\{ \int_{s_r} [-i(\hat{\mathbf{n}} \cdot \mathbf{k}_s)V_1(x) - V_2(x)] \\
& \exp(-i\mathbf{k}_s \cdot \mathbf{r})\sqrt{1 + [Z'(x)]^2}dx \\
& - \int_{s_{o1}} V_3(x)\exp(-i\mathbf{k}_s \cdot \mathbf{r})\sqrt{1 + [Z_{o1}'(x)]^2}dx \bigg\}, \quad (18)
\end{aligned}
$$

with $\mathbf{k}_s = k_0(\sin\theta_s\hat{x} + \cos\theta_s\hat{z})$. The scattering angle θ_s is defined with respect to the normal in the clockwise direction. The scattering coefficient in (17) is the total scattering cross section, accounting for both the coherent and incoherent scattering energies.

3. NUMERICAL RESULTS

3.1. Validation

Validation of the proposed method is examined by comparison with the published data [23]. Figure 2 shows bistatic scattering coefficient of a 2-D PEC cylinder of radius 1.2732λ situated on a planar ground plane under the tapered plane wave incidence. The tapering parameter g is selected as $L/4$, and length of the flat surface is $L = 40\lambda$. The number of discretisations on the ground surface and metallic cylinder's surface are $N = 512$ and $N_0 = 240$, respectively. The incident and scattering angles are $\theta_i = 0°$ and $\theta_s = -90° \sim 90°$. In reference [23], the problem is solved using the extinction theorem, and conducting ground planar is assumed. In our case, a dielectric substrate with high relative permittivity $\varepsilon_r = (1, 500)$ is assumed to represent a highly reflective surface. Two results are in good agreement as observed in Figure 2. The central peak is due to the reflection of the tapered incident wave by the flat surface.

3.2. Effect of the RMS Height of Random Rough Surface

Figure 3 shows the bistatic scattering coefficient of PEC cylinder partially embedded in a dielectric flat surface and a random dielectric rough surface respectively. The dielectric rough surface is characterized by a small rms height $h = 0.005\lambda$ and $l = 0.35\lambda$. The metallic cylinder
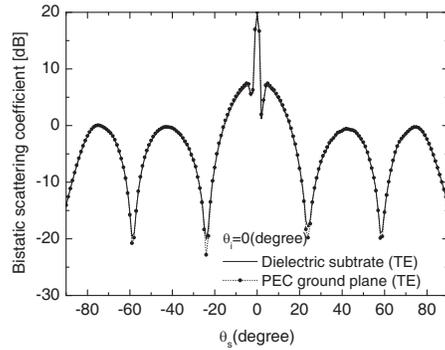
Figure 2. Bistatic scattering coefficient of a PEC cylinder located on a planar ground plane.
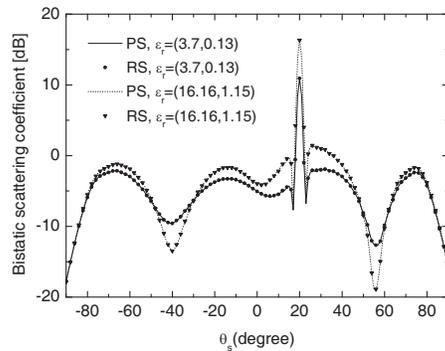
Figure 3. Bistatic scattering coefficient of a PEC cylinder partially embedded in the dielectric planar surface and the dielectric rough surface interface with small rms height, where "PS" denotes the planar surface case while "RS" represents the rough surface case.

of radius 1.0λ is located at $(x_c, z_c) = (0.0,\ 0.0)$. The length of the rough surface and tapering parameter are chosen as $L = 40\lambda$ and $g = L/4$, respectively. The region 1 is assumed as a nonmagnetic medium, $\mu_1 = \mu_0$. The numbers of discretization on the rough surface and the PEC cylinder's surface are $N = 512$ and $N_0 = 240$, respectively. The operating frequency is $1.2\,\mathrm{GHz}$. The incident and scattering angles are $\theta_i = 20°$, $\theta_s = -90° \sim 90°$. To obtain the average bistatic scattering coefficient $\langle \sigma(\theta_s) \rangle$ for the rough surface case, samples of 500 independent random rough surface realizations are used in the Monte Carlo simulation. The number of 500 independent rough surfaces chosen is able to guarantee the convergence of the bistatic scattering evaluated for the cases considered here [25]. The

above-mentioned parameters are used in the following examples unless specified otherwise.

It can be seen in Figure 3 that bistatic scattering pattern for the small rms height $h = 0.005\lambda$ and $l = 0.35\lambda$ is almost identical to that for the planar surface case. The similar phenomenon is observed for the cases of different relative dielectric constants in the lower region 1. The observed specular peak is due to its coherent wave scattering by a random rough surface with a small rms height and flat surface, respectively. More detailed explanation about this phenomenon is given in the following paragraph. The conclusion drawn from Figure 3 is that the scattering coefficients of partially buried PEC cylinder are not significantly affected by the rough surface with small rms height as compared to the flat surface case. Thus, it is reasonable to assume random rough surface as a planar surface to analysis of the electromagnetic scattering problem at VHF/UHF band. The reason is that the roughness of rough surface is less than fraction of the electromagnetic wavelength at the VHF/UHF region.

Figures 4(a) and 4(b) show the bistatic scattering coefficients for partially buried PEC cylinder with different sizes. A Gaussian random dielectric rough surface is characterized by assuming: (1) $h = 0.1\lambda$, $l = 0.5\lambda$, and (2) $h = 0.25\lambda$, $l = 0.5\lambda$, respectively. The central position of PEC cylinder is at $(x_c, z_c) = (0.0, 0.0)$. The incident angle is $\theta_i = 20°$. A sharp specular peak at $\theta_s = 20°$ is observed in the forward direction, which is due to the coherent wave scattering from a random rough surface with a small rms height in case (1). The finite angular width of forward specular peak is due to the finite length of the surface. The coherent specular peak becomes smaller as
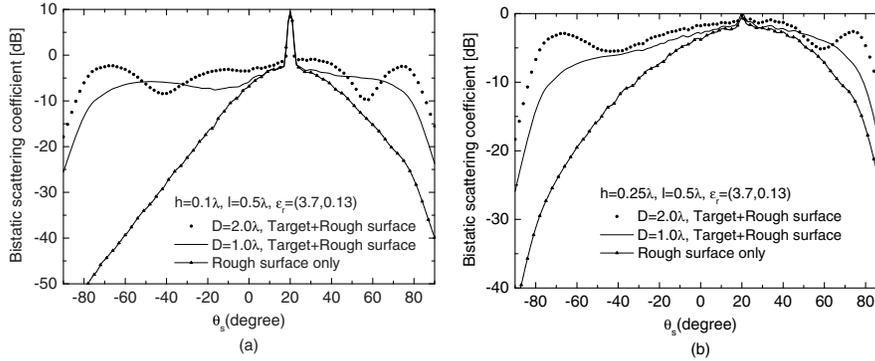
Figure 4. Bistatic scattering coefficient of a PEC cylinder partially embedded in the dielectric rough surface interface with different rms heights and different sizes of PEC cylinder.
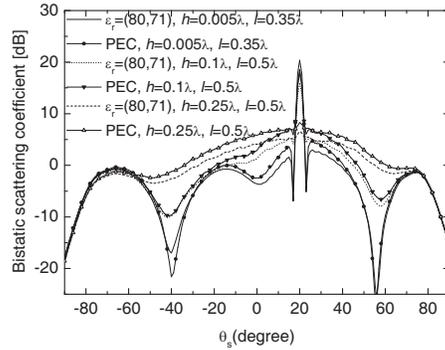
Figure 5. Bistatic scattering coefficient of a PEC cylinder partially embedded in PEC rough surface interface and the dielectric rough surface with high relative permittivity.

the rms height increases in the case (2). The reason is that the total scattering coefficient can be decomposed into two parts, the incoherent and the coherent components, $\sigma_T = \sigma_{incoh} + R_{coh} \cdot \sigma_{fs}$ [21]. σ_{incoh} is the infinite length rough surface incoherent scattering coefficient, R_{coh} is the coherent intensity reflection coefficient in the Kirchhoff approximation given by $R_{coh} = e^{-[k_0 h(\cos_i + \cos_s)]^2}$, and σ_{fs} is the finite length flat surface scattering coefficient. The cross section σ_{fs} can be evaluated numerically, this factor provides a finite angular width for the coherent component. The coherent scattered wave only exists in the specular directions for an infinite rough surface [26]. As the rms height increases, the coherent component diminishes exponentially. This is because the scattered fields from different parts of the rough surface have a large variance in phase fluctuation. The width of the specular peak was studied with measurements data in [27].

The contribution of scattering by metallic targets to the total scattered field becomes larger as the size of PEC cylinder increased. Bistatic scattering coefficients for the horizontal polarization have more peaks as a function of the scattered angle for a large size of PEC cylinder as compared to those in the vertical polarization case [20]. The phenomenon is also observed in the case of metallic cylinder situated on the ground plane, as shown in Figure 2.

3.3. Effect of Water Content in the Soil

Analyzing of the electromagnetic scattering by the composite surface, such as a ship on the ocean surface, is a very important issue in the area of microwave remote sensing. To reduce the computational
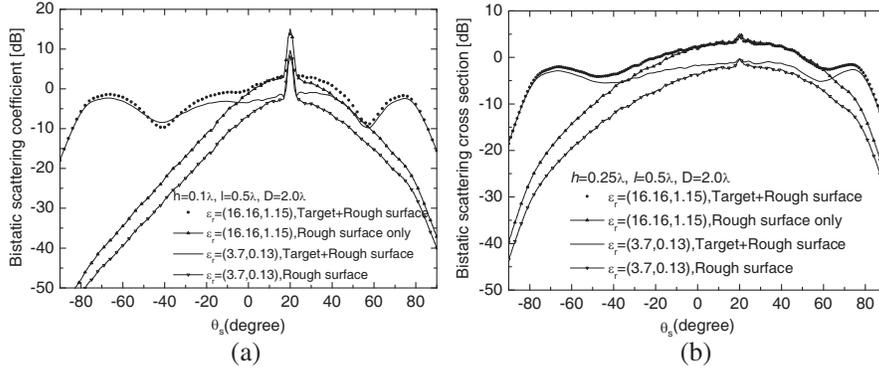
Figure 6. Bistatic scattering coefficient of a PEC cylinder partially embedded in the dielectric rough surface interface with different permittivities and different rms height of a rough surface.

complexity of the problem to be solved using the MoM, both the partially buried ship and the ocean like rough surface are usually assumed as to be metallic to decrease the number of unknowns. For the case of PEC targets partially embedded in a semi-infinite dielectric rough surface ground, the effect of water content of the soil on the scattering coefficients is required to be further investigated.

Figure 5 shows bistatic scattering coefficients of the PEC cylinder of radius 1.0λ partially buried in a metallic rough surface and a dielectric rough surface, respectively. A high relative permittivity $\varepsilon_r = (80,\ 71)$ in the lower region 1 is chosen for the case of dielectric rough surface, which is used to approximate the relative dielectric constant of sea at 1.2 GHz. The metallic cylinder is located at $(x_c, z_c) = (0.0,\ 0.0)$. Other parameters are shown in Figure 5. The incident is $\theta_i = 20°$. It can be seen that the scattering characteristic of PEC cylinder partially buried in a metallic rough surface is similar to that of metallic cylinder buried in a dielectric rough surface with the high relative dielectric constant. It demonstrates that ocean like rough surface assumed as a metallic rough surface is practical to analyze the interactions of the electromagnetic wave with PEC objects on the ocean rough surface at L band [18, 19].

Figure 6 shows the bistatic scattering coefficients of the PEC cylinder partially embedded in a dielectric rough surface as function of water content in the soil. The relative dielectric constants of the soil with water content of 5% and 30% are determined using the empirical model [24]. Their respective relative permittivity in the lower region 1 is found as $\varepsilon_r = (3.7,\ 0.13)$ and $\varepsilon_r = (16.16,\ 1.15)$, respectively. The

metallic cylinder is located at $(x_c, z_c) = (0.0, \ 0.0)$. Other parameters used are presented in Figure 6. The incident is $\theta_i = 20°$. It show that the contribution of scattering by the dielectric rough surface and the PEC cylinder to the total scattered field becomes stronger at the higher water content of the soil and the larger size of cylinder, especially in the specular forward direction. The coherent wave peak in the specular direction is observed for the case of a smaller rms height, and disappears as the rms height becomes larger, which is also observed in TM case [20]. The numerical results illustrate that the water content of the soil has significant effects on the bistatic scattering pattern. The value of scattering coefficient evaluated at large scattering angles is almost the same in the cases of different water contents of the soil. Thus, investigating of the LGA scattering from the composite rough surface with partially buried objects is an important issue in the area of microwave remote sensing and targets detection. The method proposed here with the help of the fast algorithm provides a numerical tool to study the LGA scattering by a 2-D metallic target partially embedded in a dielectric rough surface.
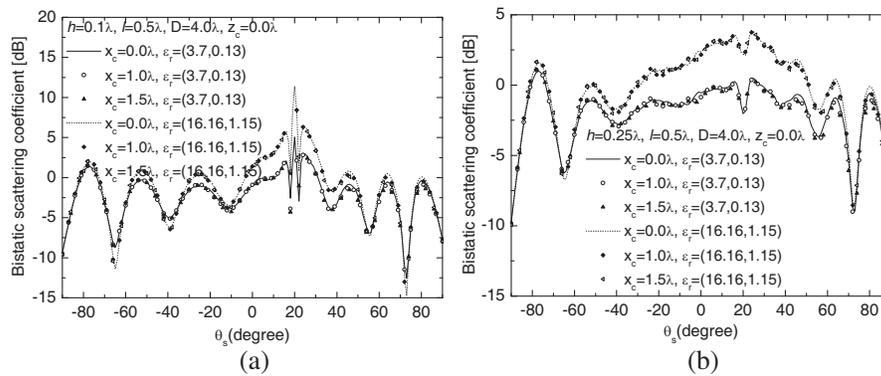
Figure 7. Bistatic scattering coefficient of a PEC cylinder partially embedded in the dielectric rough surface interface with different center locations of the PEC cylinder and different rms height of a rough surface.

Figure 7 shows bistatic scattering coefficients of PEC cylinder partially embedded in a dielectric rough surface as a function of the relative dielectric constant in region 1 and the location of PEC cylinder respectively. The metallic cylinder of radius 2.0λ is located at $(x_c, z_c) = (0.0, \ 0.0)$, $(x_c, z_c) = (1.0\lambda, \ 0.0)$ and $(x_c, z_c) = (1.5\lambda, \ 0.0)$, respectively. Results show that bistatic scattering coefficients are not significantly affected by changing location of the PEC cylinder along

the x-direction. One reason is that the size of cylinder is smaller than the length of dielectric rough surface. The other reason is that the PEC cylinder is still situated within the main beam of the tapered incident wave. Bistatic scattering coefficients become larger as the relative dielectric constant in region 1 increases, especially at the specular direction. As the rms height becomes larger, the coherent specular peak becomes smaller. This is due to that the contribution of dielectric rough surface scattering to the total scattered field becomes smaller in the specular direction, as mentioned in Section 3.2.

4. CONCLUSIONS

The MoM with pulse basis functions together with the point matching technique is applied to characterize electromagnetic scattering by a 2-D PEC cylinder partially embedded in a random dielectric rough surface interface. The total far-zone scattered fields including scattering from both a metallic cylinder and a dielectric rough surface in the upper half space are computed using the Monte Carlo simulation. The numerical results show that the rms height of a random dielectric rough surface and the water content of the soil affect significantly the scattering coefficients of partially buried PEC cylinders. The proposed method combined with the fast algorithm and parallel implementation can provide a numerical tool to characterize efficiently and accurately the LGA scattering of large size of 2-D PEC objects partially immersed in a random dielectric rough surface.

REFERENCES

1. Zhang, Y., Y. E. Yang, H. Braunisch, and J. A. Kong, "Electromagnetic wave interaction of conducting object with rough surface by hybrid SPM/MOM technique," *Progress In Electromagnetics Research*, PIER 22, 315–335, 1999.
2. Chiu, T. and K. Sarabandi, "Electromagnetic scattering interaction between a dielectric cylinder and a slightly rough surface," *IEEE Trans. Antennas Propagat.*, Vol. 47, No. 5, 902–913, May 1999.
3. Wang, X., X. Luo, Z. Zhang, and J. Fu, "The study of an electromagentic scattering model for two adjacent trunks above a rough surface ground plane," *Microwave and Optical Technology Letters*, Vol. 20, No. 6, 369–376, 1999.
4. Lawrence, D. E. and K. Sarabandi, "Electromagnetic scattering from a dielectric cylinder buried beneath a slightly rough surface,"

IEEE Trans. Antennas Propagat., Vol. 50, No. 10, 1368–1376, Oct. 2002.

5. Cottis, P. G. and J. D. Kanellopoulos, "Scattering of electromagnetic waves from cylindrical inhomogeneities embedded inside a lossy medium with sinusoidal surface," *Journal of Electromagnetic Waves and Applications*, Vol. 6, No. 4, 445–458, 1992.

6. Cottis, P. G., C. N. Vazouras, C. Kalamatianos, and J. D. Kanellopoulos, "Scattering of TM waves from a cylindrical scatterer buried inside a two-layer lossy ground with sinusoidal surface," *Journal of Electromagnetic Waves and Applications*, Vol. 10, No. 7, 1005–1021, 1996.

7. O'Neill, K., R. F. Lussky Jr, and K. D. Paulsen, "Scattering from a metallic object embedded near the randomly rough surface of a lossy dielectric," *IEEE Trans. Geosci. Remote Sensing*, Vol. 34, No. 2, 367–376, Mar. 1996.

8. Zhang, G. F., L. Tsang, and Y. Kuga, "Studies of the angular correlation function of scattering by random rough surfaces with and without a buried object," *IEEE Trans. Geosci. Remote Sensing*, Vol. 35, No. 2, 444–453, Mar. 1997.

9. Wang, X., C. F. Wang, Y. B. Gan, and L. W. Li, "Electromagnetic scattering from a circular target above or below rough surface," *Journal of Electromagnetic Waves and Applications*, Vol. 17, No. 8, 1153–1155, 2003.

10. Zhang, G. F., L. Tsang, and K. Pak, "Angular correlation function and scattering coefficient of electromagnetic waves scattered by a buried object under a two-dimensional rough surface," *J. Opt. Soc. Am. A*, Vol. 15, No. 12, 2995–3002, Dec. 1998.

11. Johnson, J. T. and R. J. Burkholder, "Coupled canonical grid/discrete dipole approach for computing scattering from objects above or below a rough interface," *IEEE Trans. Geosci. Remote Sensing*, Vol. 39, No. 6, 1215–1220, Jun. 2001.

12. El-Shenawee, M., C. Rappaport, E. Miller, and M. Silevitch, "Three-dimensional subsurface analysis of electromagnetic scattering from penetrable/PEC objects buried under rough surfaces: use of the steepest descent fast multipole method (SDFMM)," *IEEE Trans. Geosci. Remote Sensing*, Vol. 39, No. 6, 1174–1182, Jun. 2001.

13. Rao, T. C. and R. Barakat, "Plane-wave scattering by a conducting cylinder partially buried in a ground plane. 1. TM case," *J. Opt. Soc. Am. A*, Vol. 6, No. 3, 1270–1280, 1989.

14. Rao, T. C. and R. Barakat, "Plane-wave scattering by a conducting cylinder partially buried in a ground plane. 2. TE

case," *J. Opt. Soc. Am. A*, Vol. 8, No. 3, 1986–1990, 1991.

15. Hamid, A. K. and M. Hamid, "A plane electromagnetic wave scattering by a conducting sphere partially buried in a ground plane," *Journal of Electromagnetic Waves and Applications*, Vol. 14, No. 5, 615–627, 2000.

16. Xu, X. B. and C. M. Bulter, "Scattering of TM excitation by coupled and partially buried cylinders at the interface between two media," *IEEE Trans. Antennas Propagat.*, Vol. 35, No. 5, 529–538, May 1987.

17. Ling, R. T. and P. Y. Ufimtsev, "Scattering of electromagnetic waves by a metallic object partially immersed in a semi-infinite dielectric medium," *IEEE Trans. Antennas Propagat.*, Vol. 49, No. 2, 223–233, Feb. 2001.

18. Pino, M. R., L. Landesa, J. L. Rodriguez, F. Obelleiro, and R. J. Burkholder, "The generalized forward-backward method for analyzing the scattering from targets on ocean-like rough surfaces," *IEEE Trans. Antennas Propagat.*, Vol. 47, No. 6, 961–969, Jun. 1999.

19. Burkholder, R. J., M. R. Pino, and F. Obelleiro, "A Monte Carlo study of the rough surface influence on the radar scattering from two-dimensional ships," *IEEE Antennas and Propagation Magazine*, Vol. 43, No. 2, 25–33, Mar. 2001.

20. Wang, X., Y. B. Gan, and L. W. Li, "Electromagnetic scattering by partially buried PEC cylinder at the dielectric rough surface interface: TM case," *IEEE Antennas and Wireless Propagation Letters*, Vol. 2, 319–322, 2003.

21. Thorsos, E., "The validity of the Kirchhoff approximation for rough surface scattering using a Gaussian roughness spectrum," *J. Acoust. Soc. Am.*, Vol. 83, No. 1, 78–92, Jan. 1988.

22. Donohue, D. J., H. C. Ku, and D. R. Thompson, "Application of iterative moment-method solutions to ocean surface radar scattering," *IEEE Trans. Antennas. Propagat.*, Vol. 46, No. 1, 121–132, Jan. 1998.

23. Valle, P. J., F. Gonzalez, and F. Moreno, "Electromagnetic wave scattering from conducting cylindrical structures on flat substrates: Study by means of the extinction theorem," *Appl. Opt.*, Vol. 33, No. 3, 512–523, 1993.

24. Wang, J. R. and T. J. Schmugge, "An empirical model for the complex dielectric permittivity of soils as function of water content," *IEEE Trans. Geosci. Remote Sensing*, Vol. 18, No. 4, 288–295, Jul. 1980.

25. Tsang, L., J. A. Kong, K. H. Ding, and C. O. Ao, *Scattering of Electromagnetic Waves — Numerical Simulations*, John Wiley & Sons, Inc., New York, 2001.

26. Tsang, L., J. A. Kong, and R. T. Shin, *Theory of Microwave Remote Sensing*, John Wiley & Sons, Inc., New York, 1985.

27. Meister, G., A. Rothkirch, H. Spitzer, and J. Bienlein, "Width of the specular peak perpendicular to the principal plane for rough surfaces," *Appl. Opt.*, Vol. 40, No. 33, 6072–6080, Nov. 2001.

28. Wang, X., C. F. Wang, Y. B. Gan, and L. W. Li, "Electromagnetic scattering from a circular target above or below rough surface," *Progress In Electromagnetics Research*, PIER 40, 207–227, 2003.

29. Chen, H. T. and G. -Q. Zhu, "Model the electromagnetic scattering from three-dimensional PEC object buried under rough ground by MoM and modified PO hybrid method," *Progress In Electromagnetics Research*, PIER 77, 15–27, 2007.

30. Li, Z.-X., "Bistatic scattering from rough dielectric soil surface with a conducting object with arbitrary closed contour partially buried by using the FBM/SAA method," *Progress In Electromagnetics Research*, PIER 76, 253–274, 2007.